International Journal of Sustainable Energy

ISSN: 1478-6451 (Print) 1478-646X (Online) Journal homepage: https://www.tandfonline.com/loi/gsol20

Effect of the angle of oblique stagnation-point flow impinging axisymmetrically on a vertical circular cylinder with mixed convection heat transfer

Asghar B. Rahimi & Reza Bayat

To cite this article: Asghar B. Rahimi & Reza Bayat (2019) Effect of the angle of oblique stagnation-point flow impinging axisymmetrically on a vertical circular cylinder with mixed convection heat transfer, International Journal of Sustainable Energy, 38:9, 849-865, DOI: 10.1080/14786451.2019.1601628

To link to this article: https://doi.org/10.1080/14786451.2019.1601628

Published online: 10 Apr 2019.

Submit your article to this journal

Article views: 12

View related articles

View Crossmark data

Full Terms & Conditions of access and use can be found at
https://www.tandfonline.com/action/journalInformation?journalCode=gsol20

INTERNATIONAL JOURNAL OF SUSTAINABLE ENERGY
2019, VOL. 38, NO. 9, 849–865
https://doi.org/10.1080/14786451.2019.1601628

Taylor & Francis
Taylor & Francis Group

Check for updates

Effect of the angle of oblique stagnation-point flow impinging axisymmetrically on a vertical circular cylinder with mixed convection heat transfer

Asghar B. Rahimi[a] and Reza Bayat[b]

[a]Faculty of Engineering, Ferdowsi University of Mashhad, Mashhad, Iran; [b]Sama Technical and Vocational Training College, Islamic Azad University, Mashhad, Iran

ABSTRACT

Governing equations in the boundary layer induced by a steady incompressible oblique stagnation-point flow axisymmetrically impinging on a vertical constant temperature cylinder along with mixed convection heat transfer due to buoyancy forces are reduced to ODEs using similarity transformations and are solved numerically. Assuming constant strength $\bar{k}$ for the oblique flow and by changing the obliqueness angle α in between zero to 90°, solution of equations' system has been repeated at any specific value of α in the states of assisting or opposing flow. Using the resulting data, the behaviour of the flow parameters like Nusselt number, situation of streamline $\Psi = 0$ at incident point and other characteristics are found against the flow obliqueness angle. The results are presented for Reynolds numbers 0.1, 1, 10, and 100 and buoyancy parameter values of $\lambda = -1, 0, 1$ in which the heat and flow mechanisms are special cases of opposing flow, no buoyancy flow, and assisting flow, respectively.

ARTICLE HISTORY
Received 17 May 2018
Accepted 21 March 2019

KEYWORDS
Oblique stagnation-point flow; axisymmetric; vertical circular cylinder; mixed convection

Nomenclature

a	radius of cylinder
A	radial flow velocity (m/s)
B	shear flow velocity (m/s)
f, g	dimensionless velocity functions
g_g	gravitational acceleration
h	convective heat transfer coefficient
k	thermal conductivity
$\bar{k}$	free stream flow velocity (m/s)
m, n	coefficients
Nu	Nusselt number
p	dynamic pressure
Pr	Prandtl number
r	coordinate in radial direction of cylinder
Re	Reynolds number
T	temperature
T_z	temperature on cylinder wall
T_∞	free stream temperature
u, w	viscous flow's r and z-component velocity
U, W	invicsid flow's r and z-component velocity
z	coordinate in axial direction of cylinder
z_s	z-value of stagnation point

CONTACT Asghar B. Rahimi rahimiab@um.ac.ir; rahimiab@yahoo.com

© 2019 Informa UK Limited, trading as Taylor & Francis Group

α flow obliqueness angle
α_s tangent angle at incident point of stagnation line
α_{th} thermal diffusivity
β volumetric thermal expansion coefficient
η dimensionless parameter
θ dimensionless temperature function
λ mixed convection parameter
μ dynamic viscosity
ν Kinematic viscosity
ρ density
τ_w shear stress on cylinder wall
ψ_{inv} invicsid flow stream function
ψ_{vis} viscous flow stream function
ψ^* dimensionless stream function

1. Introduction

The key to the vast variety of studies being accomplished regarding the problem of stagnation- point flows on a plate or a cylinder is their wide applications in the industry. Achieving accurate results of flow behaviour in the viscous boundary layer would be possible by the use of analytical methods, especially the use of similarity solutions. However, the main challenge of this approach is finding suitable similarity variables plus finding solutions to the governing differential equations.

The two-dimensional laminar incompressible steady flow impinging perpendicularly and obliquely on a flat plate was tackled by many researchers in early nineteens. They were able to transform the governing equations into ordinary differential equations which could be solved by the use of numerical methods. This was also done for the situations in which a cylinder was stationary and or rotating. The continuing studies in twenties are reviewed here. A perturbation formulation for the heat transfer problem of an axisymmetric stagnation flow was introduced by Rahimi (2003) considering high Reynolds numbers. Another study on oblique stagnation-point flow on a circular cylinder was conducted by Weidman and Putkaradze (2003). In two separated studies, Saleh and Rahimi (2004a, 2004b, 2004c) took into account a moving cylinder with a time-dependent axial velocity and uniform suction and blowing under stagnation point-flow and heat transfer by use of similarity solutions. Also, a solution for stagnation flow and heat transfer was taken into account for a moving cylinder along with transpiration by (Rahimi 2004) using perturbation methods with high Reynolds numbers as perturbation parameter. Furthermore, Saleh and Rahimi (2005) expressed results using appropriate similarity variables for an axisymmetric radial stagnation-point flow on a cylinder with constant rotational velocity and time-dependent angular velocity. Wang (2007) used similarity solution in the problem of stagnation flow on a cylinder with axial movement and replaced partial slip condition for no-slip condition on its wall. Rotational movement with time-dependent angular velocity for cylinder was also considered by Rahimi and Saleh (2007) as continuing studies. They (2008a; 2008b) also went further to consider simultaneous axial and rotational movement along with transpiration on the problem of axisymmetric stagnation-point flow and heat transfer on the cylinder. The case of unaxisymmetric heat transfer in stagnation flow on a cylinder with simultaneous axial and rotational movements which is caused by unaxisymmetric distribution of wall temperature or wall heat flux around the cylinder's surface was also dealt with by Rahimi and Saleh (2008). The problem of time-dependent transpiration, axial and rotational movements for a cylinder by use of similarity solutions were presented by Haghighi and Rahimi (2010) in the case of axisymmetric stagnation-point flow and heat transfer. Case of compressible fluid for the problem of stagnation-point flow and heat transfer on a stationary cylinder was first brought about by Mohammadiun and Rahimi (2012) and Mohammadiun, Rahimi, and Kianifar (2013). They were successful in coming up with similarity variables while including the effect of variable density in the resulting similar equations of velocity and temperature, which should have been solved simultaneously. The problem of mixed convection heat

transfer for a vertical flat plate in both normal axisymmetric stagnation-point flow and inclined cases were recently considered by Wang and Ng (2013). The work of stagnation flow and heat transfer on a stretching/shrinking cylinder with surface permeation was presented in two papers of Najib, Bachok, and Arifin (2014), and Najib et al. (2014). The task of unaxisymmetric stagnation-point flow and heat transfer on a moving cylinder with time-dependent axial velocity and non-uniform normal suction and blowing was investigated by Alizadeh, Rahimi, and Najafi (2016). The interesting case of compressible fluid problem was further progressed by Rahimi, Mohammadiun, and Mohammadiun (2016) for the condition of axially moving cylinder. The geometry of rotating vertical cylinder in the case of three-dimensional, unsteady stagnation-point flow considering mixed convection heat transfer was numerically investigated by Bayat and Rahimi (2017a). They actually solved the three-dimensional Navier–Stokes and energy equations directly and for the first time by computational methods without employing any similarity variables. Also, the task of mixed convection heat transfer for unsteady impulsive oblique stagnation-point flow on a vertical cylinder was investigated by Bayat and Rahimi (2017b). This work shows what happens when an axisymmetric oblique stagnation-point flow starts suddenly towards a cylinder which is affected by a free convection flow, too. Variation of the flow characteristics and their distributions against the time parameter was represented in this work.

In the present analysis, the steady-state problem of mixed convection heat transfer for a vertical circular cylinder impinged by an oblique stagnation-point flow is dealt with and the effect of flow obliqueness on some characteristics is investigated. So, this problem is a new situation which includes both oblique free-stream flow and the vertical flow caused by free convection heat transfer, simultaneously. A constant velocity axisymmetric outer flow impinges on a circular cylinder, obliquely. The flow is supposed to be inviscid far from the cylinder but in the neighbourhood of the surface (boundary layer), equations of viscous flow are reduced to ODEs using similarity transformations and are solved numerically to determine velocity and temperature of the flow field. This solution is repeated for any arbitrary angle of outer flow in the range of zero to 90° for assisting or opposing buoyancy and several inclination angles.

2. Problem formulation

Axisymmetric incompressible steady-state stagnation- point flow impinges obliquely on a vertical circular cylinder with radius a and infinite length with constant wall temperature T_w in the space influenced by gravity acceleration g_g. A schematic of this problem for two states of assisting and opposing flow against buoyancy forces is presented in Figure 1. It is considered that the flow far from the cylinder has inviscid behaviour and is composed of two perpendicular flows: Normal stagnation flow onto the cylinder's surface and Shear flow parallel to the cylinder's axis. Assuming the axisymmetric coordinate system (r, z), shown in Figure 1, by referring to Weidman and Putkaradze (2003), the oblique stream function and velocity components with coefficients $A \succ o$ and $B \succ 0$ are as follows:

$$\psi_{inv} = A(r^2 - a^2)z + B\frac{1}{2a}(r^2 - a^2)^2 \tag{1}$$

$$\begin{cases} U = -\dfrac{1}{r}\dfrac{\partial \psi}{\partial z} = -A\left(r - \dfrac{a^2}{r}\right) \\ W = \dfrac{1}{r}\dfrac{\partial \psi}{\partial r} = 2Az + 2Ba\left(\dfrac{r^2}{a^2} - 1\right) \end{cases} \tag{2}$$

It is easily provable that velocity field of Equation (2) is true in the continuity equation. The strength of normal stagnation flow and axial shear flow are indicated by coefficients A and B, respectively. Their summation gives the total strength of the oblique flow $\bar{k}$, which is constant at any obliqueness

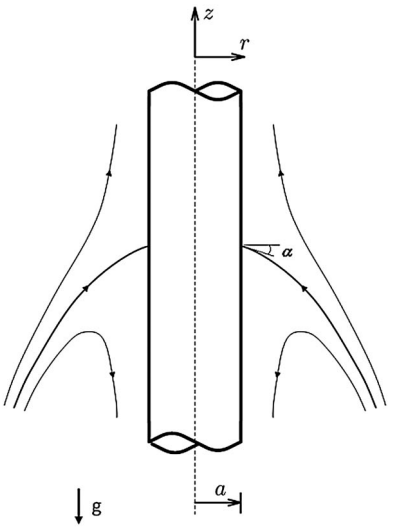

a)

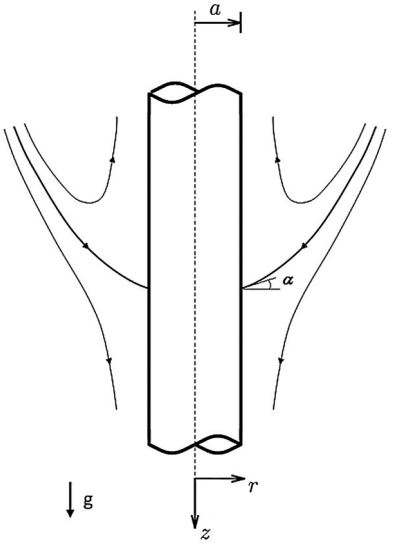

b)

Figure 1. Schematic of the inviscid oblique stagnation-point flow axisymmetrically impinging on a vertical circular cylinder at obliqueness angle a in existence of buoyancy forces; (a) assisting flow (b) opposing flow.

angle, so:

$$A + B = Const. = \bar{k} \tag{3}$$

Since the separating streamline $\psi = 0$, from Equation (1) has parabolic form, we use the tangent angle of that at the incidence point on the cylinder wall, called α, as the flow obliqueness scale. This definition, relying on the inviscid free stream flow, is used just as a scale and the correct tangent angle named as α_s has different values in practice because of the fluid viscosity effects. For considering the influence of α in equations of oblique flow velocities, constants A and B in Equation (1) must

be determined. For $\psi = 0$ at $r = a$ in Equation (1):

$$\tan\alpha = \left|\frac{dz}{dr}\right|_{\substack{\psi=0\\ r=a}} = \frac{B}{A} \tag{4}$$

Using Equations (3), and (4), we obtain:

$$A = \frac{\cos\alpha}{\sin\alpha + \cos\alpha}\bar{k}, \quad B = \frac{\sin\alpha}{\sin\alpha + \cos\alpha}\bar{k} \tag{5}$$

For finding the flow field in the laminar boundary layer (region close to the cylinder's surface), we need to obtain governing equations in this region for the purpose of solving them. These equations in the axisymmetric cylindrical coordinate system employing velocity components u (r, z) in r-direction, w (r, z) in z-direction and temperature field T (r, z) are as follows:

Mass continuity:

$$\frac{\partial}{\partial r}(ru) + r\frac{\partial w}{\partial z} = 0 \tag{6}$$

Momentum continuity (Navier–Stokes equations):

$$u\frac{\partial u}{\partial r} + w\frac{\partial u}{\partial z} = -\frac{1}{\rho}\frac{\partial p}{\partial r} + \upsilon\left(\frac{\partial^2 u}{\partial r^2} + \frac{1}{r}\frac{\partial u}{\partial r} - \frac{u}{r^2} + \frac{\partial^2 u}{\partial z^2}\right) \tag{7}$$

$$u\frac{\partial w}{\partial r} + w\frac{\partial w}{\partial z} = -\frac{1}{\rho}\frac{\partial p}{\partial z} + \upsilon\left(\frac{\partial^2 w}{\partial r^2} + \frac{1}{r}\frac{\partial w}{\partial r} + \frac{\partial^2 w}{\partial z^2}\right) \pm g_g\beta(T - T_\infty) \tag{8}$$

The last term in Equation (8) is the Boussinesq's approximation of buoyancy forces in z-direction. In that, g_g is gravitational acceleration and β is fluid volumetric thermal expansion coefficient of fluid. The positive sign indicates the gravity acceleration is in negative z-direction, then buoyancy forces are toward positive direction, i.e. flow direction, (assisting flow), whereas the minus sign indicates the condition positive z-direction gravity which makes buoyancy forces oppose the flow (opposing flow), refer to Figure 1.

Energy continuity:

$$u\frac{\partial T}{\partial r} + w\frac{\partial T}{\partial z} = \alpha_{th}\left(\frac{\partial^2 T}{\partial r^2} + \frac{1}{r}\frac{\partial T}{\partial r} + \frac{\partial^2 T}{\partial z^2}\right) \tag{9}$$

In which, α_{th} is thermal diffusivity. With respect to the no-slip condition on the cylinder's surface on the one side, and viscous flow transformation to inviscid flow far from the cylinder on the other side, the boundary conditions of the problem are, as

$$\begin{aligned} &r = a: \quad u = w = 0 \quad \text{and} \quad T = T_w \\ &r \to \infty: \begin{cases} u = U \\ w = W \end{cases} \quad \text{and} \quad T = T_\infty \end{aligned} \tag{10}$$

The viscous region stream function is considered to be

$$\psi_{vis} = Aa^2 f(\eta)z + Ba^3 g(\eta) \tag{11}$$

To transform nonlinear momentum equations to the solvable linear form, the similarity transformations for the velocity components (extracted from above equation) and temperature variable are

used as follows:

$$\begin{cases} u = -A\,a\eta^{-\frac{1}{2}} f(\eta) \\ w = 2Af'(\eta)z + 2Bag'(\eta) \\ \dfrac{T - T_\infty}{T_w - T_\infty} = \theta(\eta) \end{cases}, \quad \eta = \left(\frac{r}{a}\right)^2 \tag{12}$$

Continuity Equation (6) is satisfied by the above-mentioned similarity variables, automatically. Eliminating the pressure term from Equations (7) and (8) yields a system of ODE as

$$\begin{cases} \eta f''' + f'' + m\,\mathrm{Re}[1 + ff'' - f'^2] = 0 \\ \eta g''' + g'' + m\,\mathrm{Re}[fg'' - f'g'] + \dfrac{\lambda}{n}\theta = 0 \\ \eta\theta'' + [1 + m\,\mathrm{Re}\,\mathrm{Pr}\,f]\theta' = 0 \end{cases} \tag{13}$$

Which m, n and other dimensionless parameters such as Reynolds number, Prandtl number and mixed convection parameter λ have the following definitions:

$$\begin{aligned} m &= \frac{\cos\alpha}{\sin\alpha + \cos\alpha}, \quad n = \frac{\sin\alpha}{\sin\alpha + \cos\alpha} \quad 0 < \alpha < 90^\circ \\ \mathrm{Re} &= \frac{a^2\bar{k}}{2\upsilon}, \quad \mathrm{Pr} = \frac{\upsilon}{\alpha_{th}}, \quad \lambda = \pm\frac{g_g\beta a(T_w - T_\infty)}{8\upsilon\bar{k}} \end{aligned} \tag{14}$$

Also, by considering Equation (10) the following boundary conditions for ODEs system (13) are obtained:

$$\begin{cases} f(1) = 0, & f'(1) = 0, & f'(\infty) = 1 \\ g(1) = 0, & g'(1) = 0, & g''(\infty) = 1 \\ \theta(1) = 1, & \theta(\infty) = 0 \end{cases} \tag{15}$$

It is notable that the first two equations in (13) with $\lambda = 0$ are exactly the same ones presented by Weidman and Putkaradze (2003) as Equations (2.11.a) and (2.11.b). Since they defined the Reynolds number based on the normal flow strength, then it is replaced by the term ($m.\ Re$) here. This is a verification of our results in an exact form.

Using the resulting data of functions f, g and θ, it is possible to calculate some flow characteristics; Nusselt number and wall shear-stress can be obtained from the below relations:

$$Nu = \frac{ha}{2k} = \frac{-k\left[\dfrac{\partial T}{\partial r}\right]_{r=a} \times a}{2k(T_w - T_\infty)} = -\theta'(1) \tag{16}$$

$$\tau_w = \mu\left(\frac{\partial w}{\partial r}\right)_{r=a} = 4\mu\bar{k}\left[mf''(1)\frac{z}{a} + ng''(1)\right] \tag{17}$$

The position where the separation streamline meets the cylinder's surface, z_s, with the shear- stress equal to zero, and the slope of this streamline at the incident point, $tg\alpha_s$, are calculated by

$$z_s = z|_{\tau_w = 0} = -a\tan\alpha\frac{g''(1)}{f''(1)} \tag{18}$$

$$tg\alpha_s = \left[\left(\frac{dz}{dr}\right)_{\psi_{vis}=0}\right]_{r=a} = -\frac{2}{3}tg\alpha\left[\frac{m\,\mathrm{Re}\,g''(1) + \dfrac{\lambda}{n}f''(1)}{f''^2(1)}\right] \tag{19}$$

Also, it is clear that for $\lambda = 0$, the two above equations are exactly identical with relations pointed by (4.2) and (4.4) in Weidman and Putkaradze (2003), respectively. This is again another way to verify results obtained in our study.

Finally, dimensionless stream functions for inviscid and viscous regions can be rewritten as follows:

$$\psi^*_{inv} = \frac{\psi_{inv}}{\bar{k}a^3} = m(\eta - 1)\frac{z}{a} + \frac{1}{2}n(\eta - 1)^2 \tag{20}$$

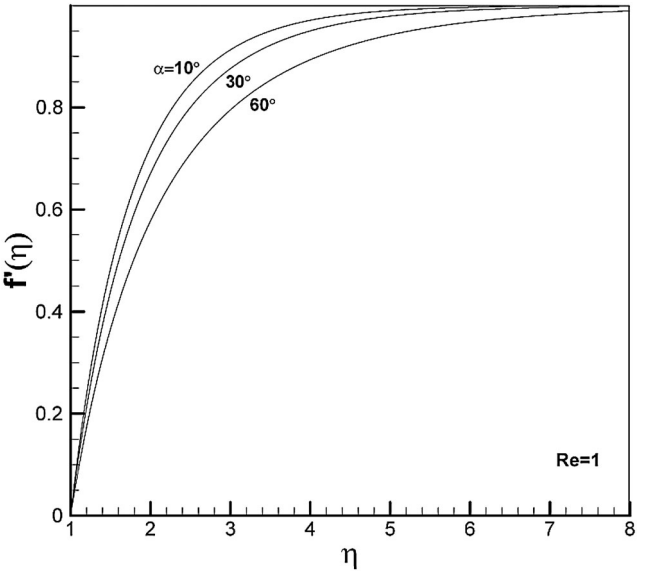

Figure 2. Distribution of radial velocity function $f'(\eta)$ for $Re = 1$ and different obliqueness angles $\alpha = 10°, 30°, 60°$.

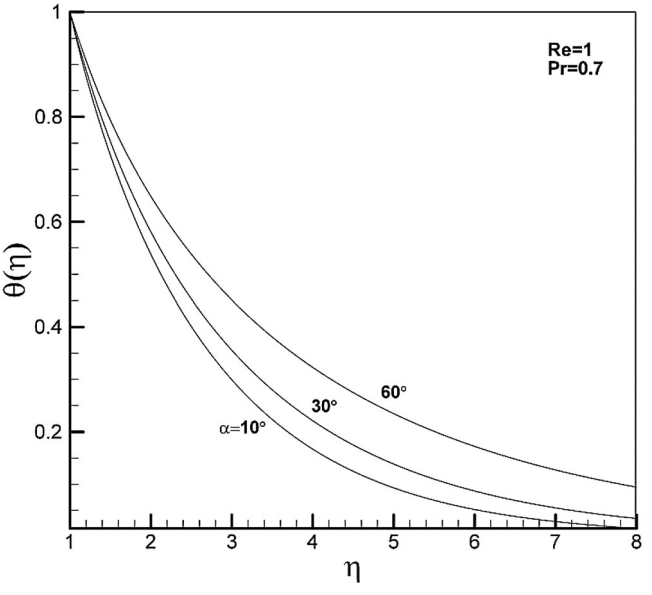

Figure 3. Distribution of thermal function $\theta(\eta)$ for $Re = 1$, $Pr = 0.7$ and different obliqueness angles $\alpha = 10°, 30°, 60°$.

$$\psi^*_{vis} = \frac{\psi_{vis}}{\bar{k}a^3} = mf(\eta)\frac{z}{a} + ng(\eta) \tag{21}$$

3. Solution and results

The ODEs system (13) along with the boundary conditions expressed by Equations (15), has been solved for two constants $Pr = 0.7$ and $\lambda = \pm 1$ in the range of $0 < \alpha < 90°$. For this purpose, the

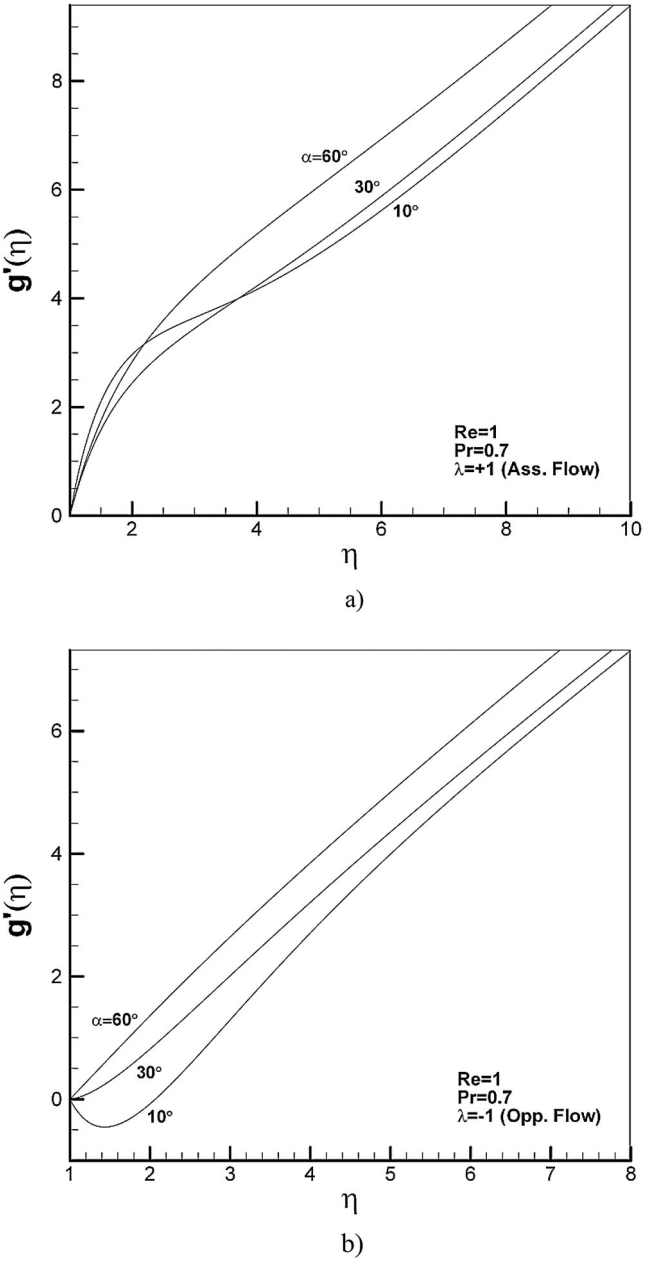

Figure 4. Distribution of axial velocity function $g'(\eta)$ for $Re = 1$, $Pr = 0.7$and different obliqueness angles $\alpha = 10°, 30°, 60°$; (a) assisting flow (b) opposing flow.

fourth-order Runge–Kutta method has been used and correct initial values for $f''(1)$, $\theta'(1)$ and $g''(1)$ have been found using a shooting method algorithm up to 13th decimal place accuracy.

Distribution of the radial velocity function $f'(\eta)$ for $Re = 1$ which is obtained for three sample angles, $\alpha = 10°$, 30°, 60° are shown in Figure 2. Distribution of thermal function $\theta(\eta)$ is depicted in Figure 3 for $Re = 1$ and $Pr = 0.7$. According to these diagrams, when obliqueness angle α increases, the range of variation of f' and θ (velocity and thermal boundary layer) increase too. This comes from reduction of the normal flow strength.

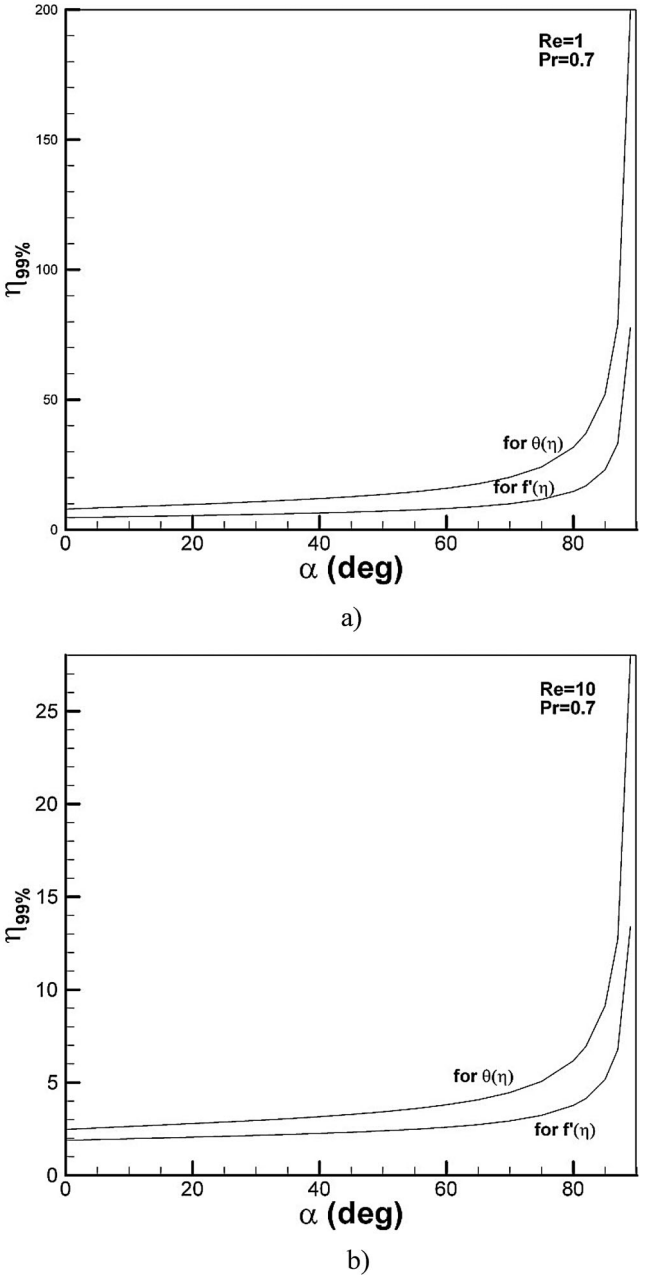

Figure 5. Variation of boundary layer thickness $\eta_{99\%}$ based on distribution of $f'(\eta)$ and $\theta(\eta)$ for constant value of $Pr = 0.7$; (a) $Re = 1$ (b) $Re = 10$.

Distribution of the axial velocity function $g'(\eta)$ for $Re = 1$, $Pr = 0.7$ and same angles in two cases of assisting and opposing flow are presented in Figure 4. The curve convexity at initial part of the diagrams in Figure 4(a) is due to the buoyancy forces acting in direction of shear flow along the cylinder's axis. Because of the reinforcing effect of buoyancy forces on assisting flow, especially for small values of α, the convexity is toward positive side too, but in the case of the opposing flow, it is towards the negative z. For larger values of α, the amount of convexity decreases because of increasing shear flow strength and elimination of the buoyancy effects.

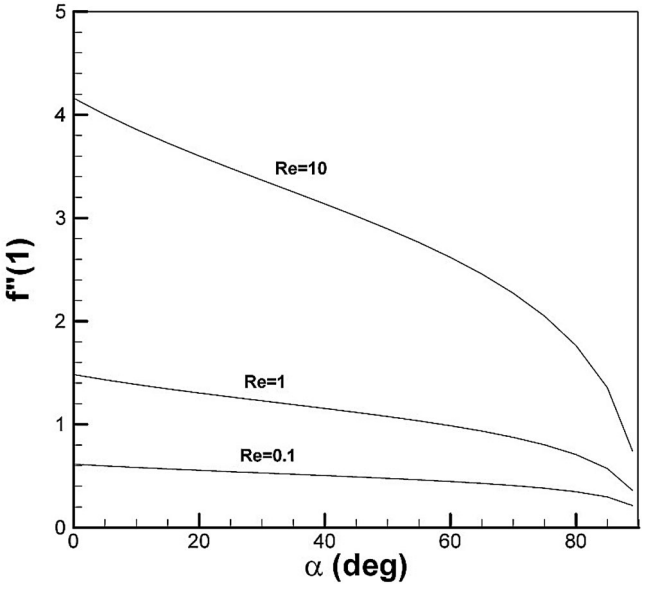

Figure 6. Variation of boundary value $f''(1)$ against obliqueness angle a for $Re = 0.1, 1, 10$.

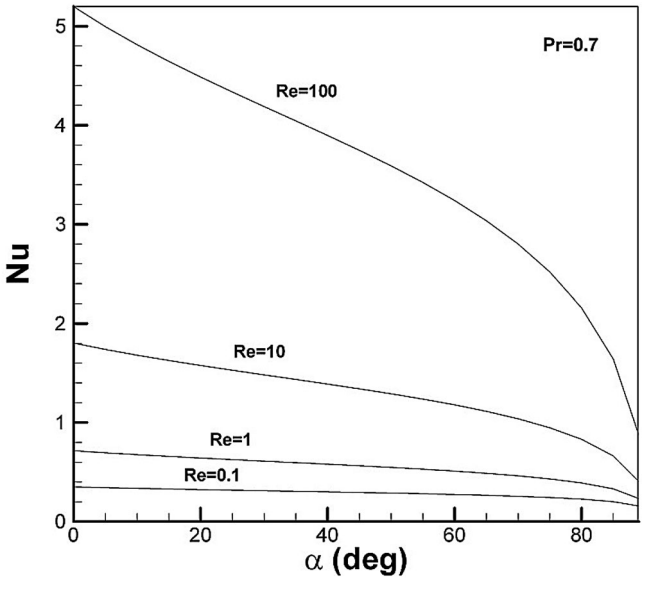

Figure 7. Variation of Nusselt number against obliqueness angle a, for $Re = 0.1, 1, 10, 100$.

The diagrams in Figure 5 are related to the variation of boundary layer thickness according to the distribution of functions $f'(\eta)$ or $\theta(\eta)$ which are drawn for $Re = 1, 10$. The quantity $\eta_{99\%}$ denoted the value of η where the value of function gains 99% of its target. According to the diagrams, from obliqueness angle about 80°, the variation of boundary layer thickness grows rapidly. Besides, in larger Reynolds numbers, we witness boundary layer with less thickness for both functions $f'(\eta)$ and $\theta(\eta)$. Another point in diagrams is the greater thermal boundary layer in proportion to dynamic boundary layer at any angle α.

The variation of boundary value $f''(1)$ against obliqueness angle for Re = 0.1, 1, 10 is observed in Figure 6. Also, the same variation for $\theta'(1)$, which is equal to Nusselt number by applying a minus

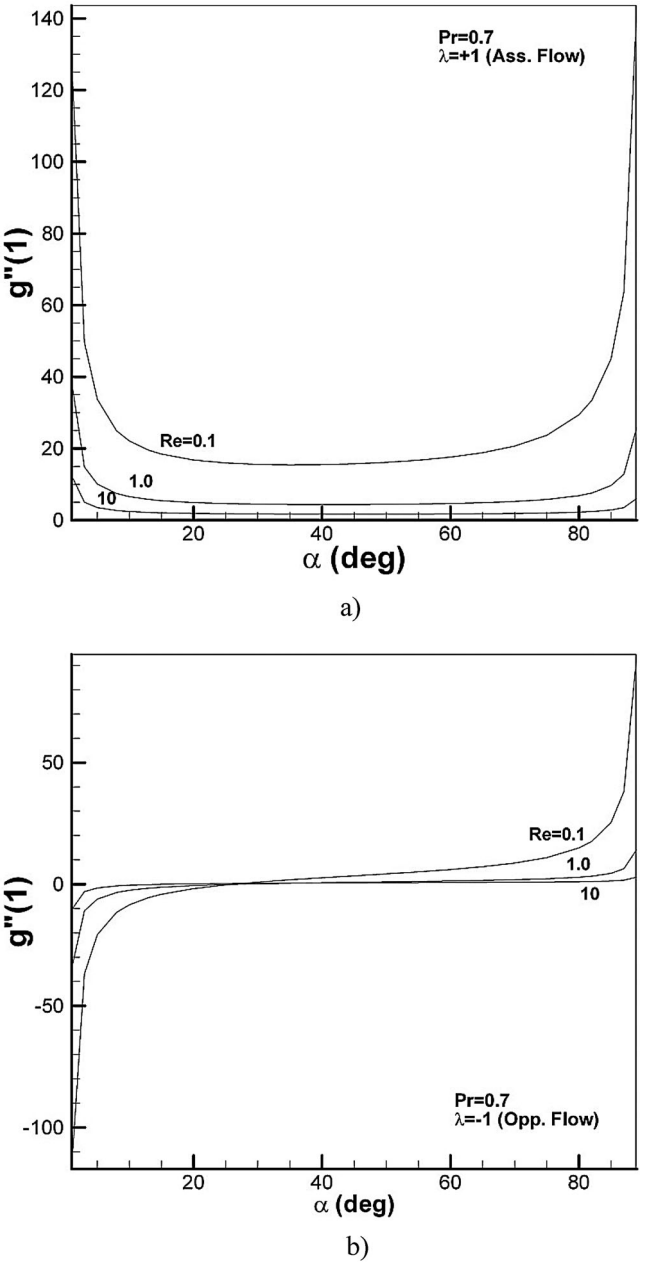

Figure 8. Variation of boundary value $g''(1)$ against obliqueness angle a for $Re = 0.1, 1, 10$; (a) assisting flow, (b) opposing flow.

sign is shown in Figure 7. According to the recent diagram, Nusselt number decreases when α increases and experiences a severe drop from an angle about 70°. Moreover, Nusselt number becomes larger for larger Reynolds numbers at any arbitrary angel α.

The variations of the boundary value $g''(1)$ against obliqueness angle for $Re = 0.1, 1, 10$ and constant values $pr = 0.7$ and $\lambda = 1$ in both states of assisting and opposing flow are shown in Figure 8. According to the diagrams, the value of $g''(1)$ in both sides of α's with the range of ($\alpha < 10°$ and $\alpha > 80°$), approximately, faces severe variations. It is seen from diagram 8-b that $g''(1)$ changes sign from negative to positive at obliqueness angle about 25° for opposing flow case and specific Reynolds numbers.

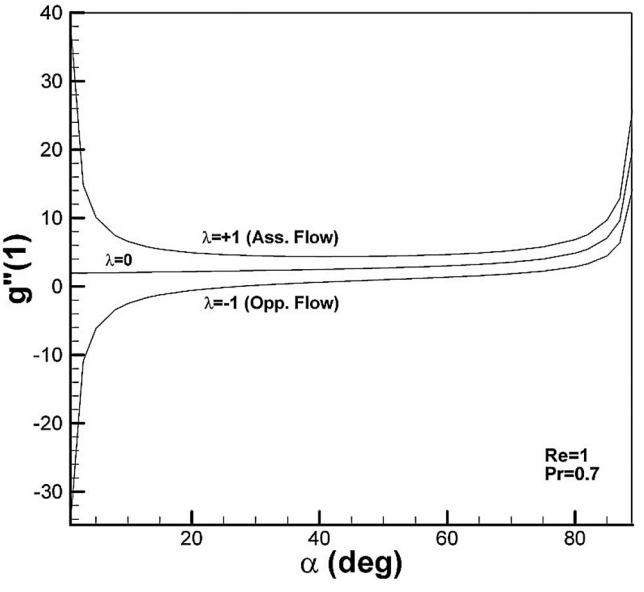

a)

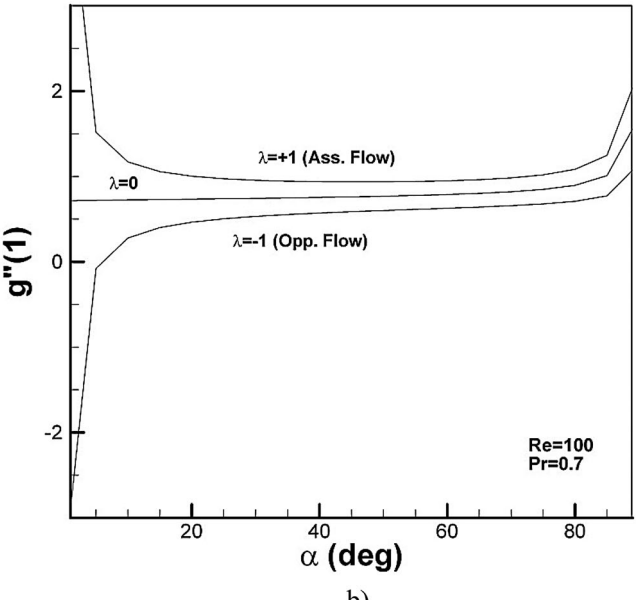

b)

Figure 9. Variation of boundary value $g''(1)$ against obliqueness angle α for, $Pr = 0.7$ and different conditions of buoyancy forces $\lambda = -1, 0, +1$, (a) $Re = 1$, (b) $Re = 100$.

A comparison of variation of the boundary value $g''(1)$ against obliqueness angle for assisting flow ($\lambda = 1$), opposing flow ($\lambda = -1$) and no-buoyancy flow ($\lambda = 0$) with constant values of $Re = 1$ and $Pr = 0.7$ is depicted in Figure 9. As it is observed, by increasing α all the three diagrams behave similarly and the curves converge to themselves. This behaviour is because of increasing shear flow contribution against normal flow which causes buoyancy forces to weaken. But at angles near to zero, because of buoyancy forces effect on the shear velocity function $g'(\eta)$, a contrary behaviour of two diagrams for assisting and opposing cases are seen. The same trend is observed for Re = 100 in Figure 9(b). So, the variations of $f''(1)$ and $g''(1)$ with incident angle affects the shear stress and the position of the incident point of separating streamline on the cylinder surface directly.

In Figure 10, four streamline patterns for the cases of inviscid flow, viscous flow with no buoyancy forces ($\lambda = 0$), viscous flow with assisting buoyancy forces ($\lambda = 1$) and viscous flow with opposing buoyancy forces ($\lambda = -1$) are drawn, respectively, for a specific obliqueness angle $\alpha = 10°$. Besides, all separating streamlines $\Psi = 0$ for these mentioned cases are drawn in Figure 11 to facilitate their comparison. According to streamline pattern in Figure 10(b), for no-buoyancy viscous flow, we witness displacement of incident point toward opposite side (negative z-direction) which is due to the no-slip condition on the cylinder wall and laminar flow in the vicinity of the wall.

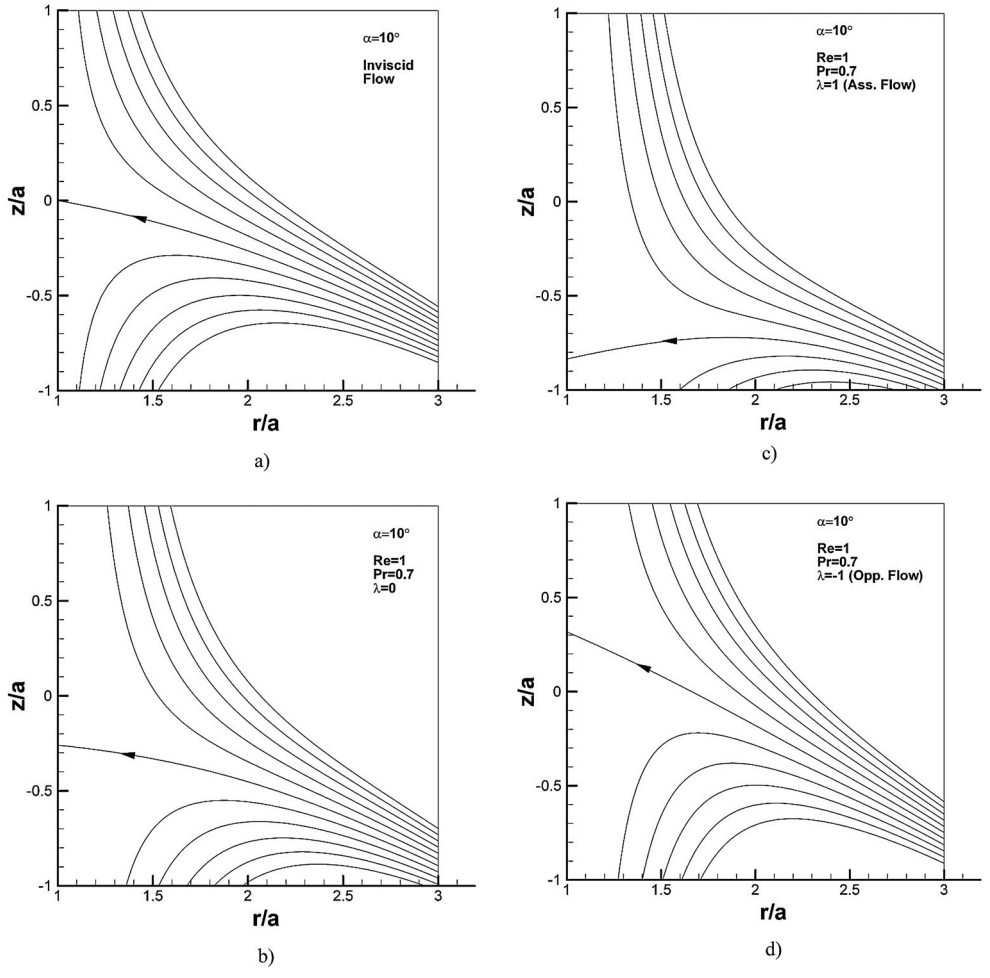

Figure 10. Streamline patterns for obliqueness angle $\alpha = 10°$ in dimensionless coordinate system (r, z); (a) inviscid flow (b) viscous flow without buoyancy forces, $\lambda = 0$ (c) viscous flow with assisting buoyancy forces, $\lambda = 1$ (d) viscous flow with opposing buoyancy forces, $\lambda = -1$.

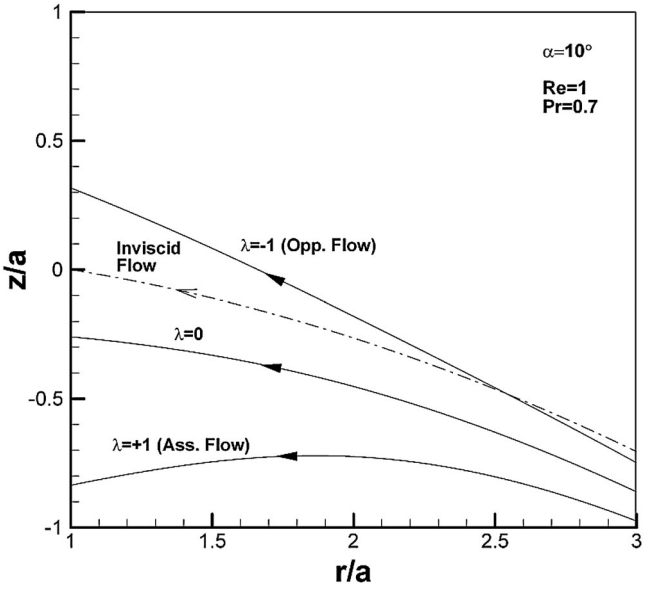

Figure 11. Comparison of separating streamline ($\Psi = 0$) with obliqueness angle $\alpha = 10°$ for different flows $\lambda = -1, 0, 1$ in dimensionless coordinate system (r, z).

According to patterns of Figure 10(c) and 10(d), the existence of mixed convection heat transfer (buoyancy forces) in the case of assisting flow, causes more displacement of incident point toward opposite side whereas opposing buoyancy forces, shift this point to accordant side (positive z-direction).

The variations of the position of separating streamline incident point, z_s and its tangent line angle, α_s against obliqueness angle α for constant values $Re = 1$, 100 and $Pr = 0.7$ for three cases of $\lambda = -1$, 0, 1 are presented in Figures 12 and 13. Regarding opposing flow case, it is observed in Figure 12 that for small values of α, the buoyancy forces shift the incident point to the positive side of z-axis, however, this point for the flow without buoyancy forces ($\lambda = 0$) is placed in the negative side. This regime continues until a specific value of α (here about 27°) and by more increase in angle, z_s it finally moves to the opposite side of the flow. For the tangent angle α_s, according to Figure 13, we see this angle in both cases of no-buoyancy flow and assisting flow always in the same direction to α and the effect of buoyancy forces just causes its value to become greater than that of the flow without buoyancy.

In the case of the assisting flow, the buoyancy forces shift the incident point to the negative side of z-axis compared to the flow with no buoyancy, as it can be seen in Figure 12. Angle α_s for this flow case, according to Figure 13, changes sign by increasing α. It means that in small values of α, the direction of separating streamline is downward (negative z) and from a specific limit on (here about 27°) its direction inclines upward due to more reduction of the buoyancy forces.

4. Conclusions

The steady-state problem of mixed convection heat transfer from a vertical cylinder under impingement of an axisymmetric oblique stagnation-point flow has been studied here with consideration of the effect of flow obliqueness angle on the characteristics of its boundary layer. In the boundary layer region near the cylinder's surface, nonlinear equations of viscous flow have been reduced to ODEs using similarity transformations and have been solved using the numerical forth order Rung–Kutta method. Since the outer flow is with constant strength, the solution process has been repeated for any arbitrary angle of obliqueness, in between zero (net normal stagnation

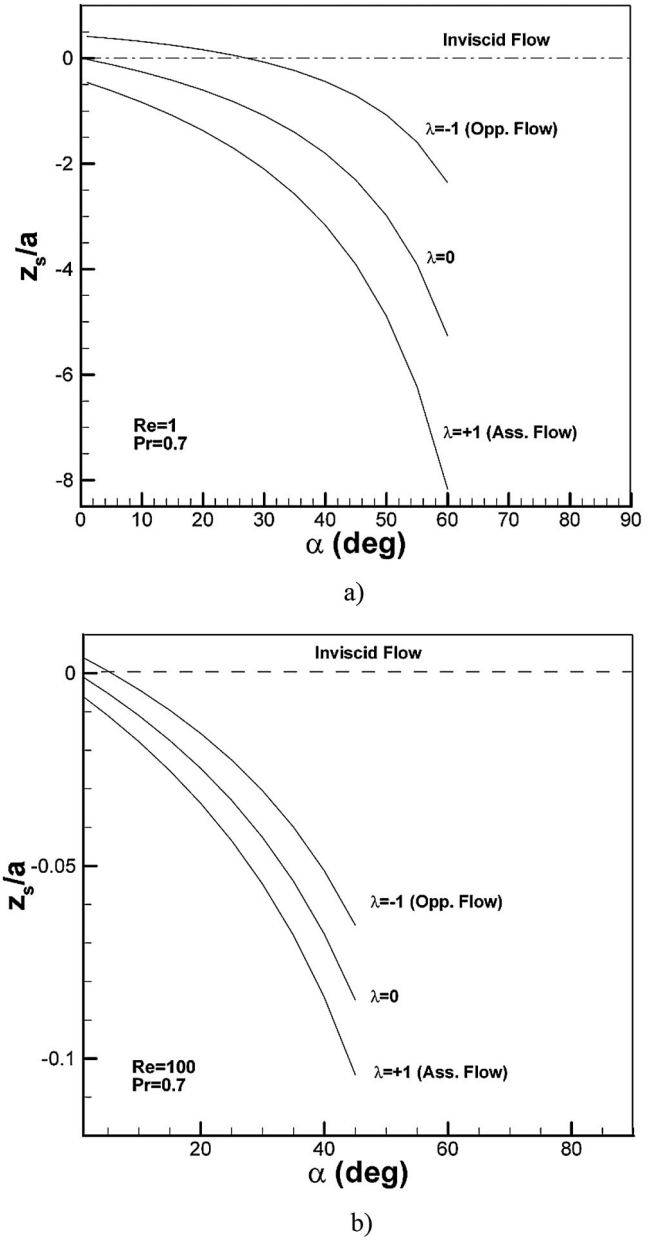

Figure 12. Variation of position of the incident point of separating streamline against obliqueness angle *a* for constant values, *Pr* = 0.7 and different flows with $\lambda = -1, 0, 1$, (a) Re = 1, (b) Re = 100.

flow) to about 90° (net axial flow) in the cases of assisting in or opposing to buoyancy forces. The computational obtained results of the problem indicate variation of different parameters such as Nusselt number, boundary value of dimensionless axial and radial velocity functions, angle and position of streamline separation, etc. against flow obliqueness angle. Based on the resulting figures, the boundary value of axial velocity function and Nusselt number decrease by increasing the angle of obliqueness α, whereas, the boundary value of radial velocity function has an abrupt grows in both sides of *the range of* α. For assisting flow case this quantity *reaches* $+\infty$ as $\alpha \to 0$ or $\alpha \to 90°$, but in opposing flow case it reaches $-\infty$ as $\alpha \to 0$ and *asymptotes to* $+\infty$ as $\alpha \to 90°$, so there is

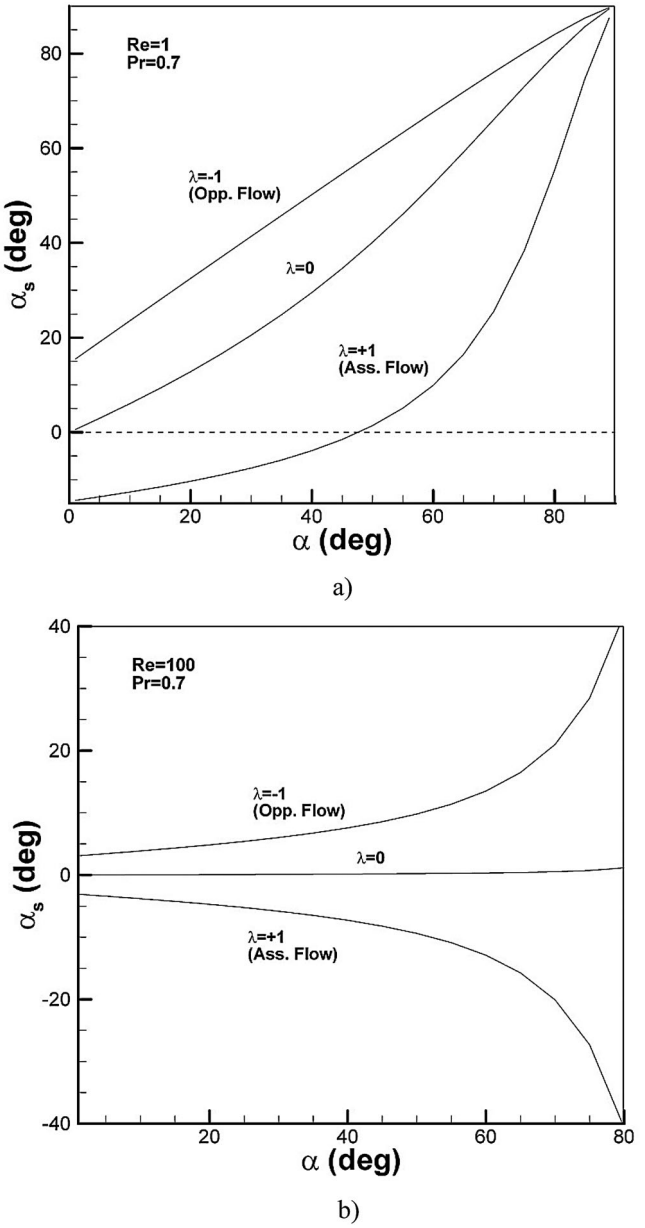

Figure 13. Variation of tangent angle of the separating streamline at incident point against obliqueness angle a for constant values, $pr = 0.7$ and different flows with $\lambda = -1, 0, 1$, (a) $Re = 1$, (b) $Re = 100$.

a specific value of α where this quantity is zero. Incident streamline tangent angle α_s for three cases of assisting flow, opposing flow and no-buoyancy flow increases against α, however, this ascension behaviour for assisting flow, starts from negative values (which means opposed direction to α), becomes zero and extends to positive side. The position of streamline incident point z_s of assisting flow is greater than that of no-buoyancy flow, both of them located in negative side, and their value grows against α. This parameter initially has positive value for opposing flow and reaches to zero and then takes negative values by increasing α. So, the variations of initial values of axial and radial velocity functions with incident angle affects the shear stress and the position of the incident point of separating streamline on the cylinder surface directly.

Disclosure statement

No potential conflict of interest was reported by the authors.

References

Alizadeh, R., A.B. Rahimi, and M. Najafi. 2016. "Unaxisymmetric Stagnation-Point Flow and Heat Transfer of a Viscous Fluid on a Moving Cylinder with Time-Dependent Axial Velocity." *Journal of the Brazilian Society of Mechanical Sciences and Engineering* 38 (1): 85–98.

Bayat, R., and A.B. Rahimi. 2017a. "Numerical Solution of Three-Dimensional N-S Equations and Energy in the Case of Unsteady Stagnation-Point Flow on a Rotating Vertical Cylinder." *International Journal of Thermal Sciences* 118: 386–396.

Bayat, R., and A.B. Rahimi. 2017b. "Unsteady Impulsive Oblique Stagnation-Point Flow Impinging Axisymmetrically on a Vertical Circular Cylinder with Mixed Convection Heat Transfer." *Scientia Iranica* 24 (4): 1966–1974.

Haghighi, B., and A.B. Rahimi. 2010. "Effect of Time-Dependent Transpiration on Axisymmetric Stagnation-Point Flow and Heat Transfer of a Viscous Fluid on a Moving Circular Cylinder." *Energy* 2 (3): 4.

Mohammadiun, H., and A.B. Rahimi. 2012. "Stagnation-Point Flow and Heat Transfer of a Viscous, Compressible Fluid on a Cylinder." *Journal of Thermo-Physics and Heat Transfer* 26 (3): 494–502.

Mohammadiun, H., A.B. Rahimi, and A. Kianifar. 2013. "Axisymmetric Stagnation-Point Flow and Heat Transfer of a Viscous, Compressible Fluid on a Cylinder with Constant Heat Flux." *Scientia Iranica* 20 (1): 185–194.

Najib, N., N. Bachok, and N.M. Arifin. 2014. "Stagnation Point Flow Over a Stretching/Shrinking Cylinder with Prescribed Surface Heat Flux." Paper presented at the Proceedings of the 3RD International Conference on Mathematical Sciences.

Najib, N., N. Bachok, N. Arifin, and A.M. Ishak. 2014. "Boundary Layer Stagnation Point Flow and Heat Transfer Past a Permeable Exponentially Shrinking Cylinder." *International Journal of Mathematical Models and Methods in Applied Sciences* 8 (1): 121–126.

Rahimi, A.B. 2003. "Heat Transfer in an Axisymmetric Stagnation Flow at High Reynolds Numbers on a Cylinder Using Perturbation Techniques." *Scientia Iranica* 10 (1): 116–121.

Rahimi, A.B. 2004. "Stagnation Flow and Heat Transfer on a Moving Cylinder with Transpiration and High Reynolds Numbers." *Iranian Journal of Science and Technology-Transaction B: Engineering* 28: 453–466.

Rahimi, A.B., H. Mohammadiun, and M. Mohammadiun. 2016. "Axisymmetric Stagnation Flow and Heat Transfer of a Compressible Fluid Impinging on a Cylinder Moving Axially." *Journal of Heat Transfer* 138 (2): 022201.

Rahimi, A.B., and R. Saleh. 2007. "Axisymmetric Stagnation—Point Flow and Heat Transfer of a Viscous Fluid on a Rotating Cylinder with Time-Dependent Angular Velocity and Uniform Transpiration." *Journal of Fluids Engineering* 129 (1): 106–115.

Rahimi, A.B., and R. Saleh. 2008a. "Similarity Solution of Unaxisymmetric Heat Transfer in Stagnation-Point Flow on a Cylinder with Simultaneous Axial and Rotational Movements." *Journal of Heat Transfer* 130 (5): 054502.

Rahimi, A.B., and R. Saleh. 2008b. "Unaxisymmetric Heat Transfer in the Axisymmetric Stagnation-Point Flow of a Viscous Fluid on a Cylinder with Simultaneous Axial and Rotational Movement Along with Transpiration." *Scientia Iranica* 15 (3): 366–377.

Saleh, R., and A.B. Rahimi. 2004a. "Axisymmetric Stagnation Point Flow of a Viscous Fluid on a Moving Cylinder with Time Dependent Axial Velocity." *International Journal of Engineering* 17 (1): 8.

Saleh, R., and A.B. Rahimi. 2004b. "Axisymmetric Stagnation-Point Flow and Heat Transfer of a Viscous Fluid on a Moving Cylinder with Time-Dependent Axial Velocity and Uniform Transpiration." *Journal of Fluids Engineering* 126 (6): 997–1005.

Saleh, R., and A.B. Rahimi. 2004c. "Stagnation-Point Flow and Heat Transfer on a Moving Cylinder with Transpiration and High Reynolds Numbers Consideration." *Iranian Journal of Science and Technology* 28 (B4): 453–466.

Saleh, R., and A.B. Rahimi. 2005. "Axisymmetric Radial Stagnation-Point Flow of a Viscous Fluid on a Rotating Cylinder with Time-Dependent Angular Velocity." *Scientia Iranica* 12 (4): 329–337.

Wang, C. 2007. "Stagnation Flow on a Cylinder with Partial Slip—An Exact Solution of the Navier–Stokes Equations." *IMA Journal of Applied Mathematics* 72 (3): 271–277.

Wang, C.Y., and C.O. Ng. 2013. "Stagnation Flow on a Heated Vertical Plate with Surface Slip." *Journal of Heat Transfer* 135 (7): 074505.

Weidman, P.D., and V. Putkaradze. 2003. "Axisymmetric Stagnation Flow Obliquely Impinging on a Circular Cylinder." *European Journal of Engineering B. Fluids* 22: 121–131.